

## Diel Migrations of Microorganisms within a Benthic, Hypersaline Mat Community

FERRAN GARCIA-PICHEL,<sup>1,2\*</sup> MARGARET MECHLING,<sup>1</sup> AND RICHARD W. CASTENHOLZ<sup>1</sup>

*Department of Biology, University of Oregon, Eugene, Oregon 97403,<sup>1</sup> and Max Planck  
Institute for Marine Microbiology, 28359 Bremen, Germany<sup>2</sup>*

Received 2 September 1993/Accepted 14 February 1994

We studied the diel migrations of several species of microorganisms in a hypersaline, layered microbial mat. The migrations were quantified by repeated coring of the mat with glass capillary tubes. The resulting minicores were microscopically analyzed by using bright-field and epifluorescence (visible and infrared) microscopy to determine depths of coherent layers and were later dissected to determine direct microscopic counts of microorganisms. Microelectrode measurements of oxygen concentration, fiber optic microprobe measurements of light penetration within the mat, and incident irradiance measurements accompanied the minicore sampling. In addition, pigment content, photosynthesis and irradiance responses, the capacity for anoxygenic photosynthesis, and gliding speeds were determined for the migrating cyanobacteria. Heavily pigmented *Oscillatoria* sp. and *Spirulina* cf. *subsalsa* migrated downward into the mat during the early morning and remained deep until dusk, when upward migration occurred. The mean depth of the migration (not more than 0.4 to 0.5 mm) was directly correlated with the incident irradiance over the mat surface. We estimated that light intensity at the upper boundary of the migrating cyanobacteria was attenuated to such an extent that photoinhibition was effectively avoided but that intensities which saturated photosynthesis were maintained through most of the daylight hours. Light was a cue of paramount importance in triggering and modulating the migration of the cyanobacteria, even though the migrating phenomenon could not be explained solely in terms of a light response. We failed to detect diel migration patterns for other cyanobacterial species and filamentous anoxyphotobacteria. The sulfide-oxidizing bacterium *Beggiatoa* sp. migrated as a band that followed low oxygen concentrations within the mat during daylight hours. During the nighttime, part of this population migrated toward the mat surface, but a significant proportion remained deep.

Compact, usually laminated microbial mats are known from hot springs, from hypersaline and other extreme contemporary habitats, and from more widespread shallow marine ecosystems of the Proterozoic. Extant mats have received considerable study in recent years, not only because they facilitate investigations of biogeochemical cycling and organismal biology and interactions on a small scale, but also because of their paleobiological implications.

Microbial mats are usually organized into distinct layers. Typically, cyanobacteria comprise the surface accreting layer, which is often less than a few millimeters thick. Thin layers of anoxygenic phototrophs, such as purple sulfur bacteria or *Chloroflexus*-related filamentous forms, underlie the cyanobacteria (7, 8, 23, 27, 30). In addition, remains of phototrophic microorganisms, presumably inactive, are found in deeper layers of the mat where little or no photosynthetically active radiation penetrates. Nonphotosynthetic, sulfide-oxidizing bacteria such as *Beggiatoa* sp. or *Thiovulum* sp. may also form specific bands (18, 24, 25). In marine mats, a thick black layer of metal sulfides may appear at some depth due to the activity of sulfate- or sulfur-reducing bacteria.

Because of the compact nature of these ecosystems, biological processes such as photosynthesis, respiration, fermentation, and sulfate-sulfur reduction create very steep gradients in the concentrations of oxygen, soluble sulfide, hydrogen ions, and other chemical species (7, 8, 35). In addition, gradients of both light intensity and spectral distribution are created due to

strong absorption and scattering of incident radiation (17, 19, 21, 31, 32). All of these gradients may change dramatically with diel periodicity, exposing the organisms to potentially harmful conditions (e.g., sulfide usually strongly inhibits oxygenic photosynthesis, oxygen is often poisonous to anaerobic microorganisms, and strong solar irradiance results in photodamage). In order to optimize fitness and competitive ability in the presence of significant diel changes, microorganisms may develop either avoidance or defense mechanisms. Metabolic versatility, in order to exploit different environmental conditions, is also ecologically important. One mechanism for optimizing fitness in the presence of dynamic gradients is migratory behavior, which may allow organisms to follow and benefit from optimal conditions within a gradient, to avoid its extreme values, or both. Migratory behavior within mats occurs in both photosynthetic and nonphotosynthetic microorganisms (3–5, 25, 28, 36, 40). In situ studies have relied heavily on qualitative observations of migratory patterns, and most studies have merely demonstrated the presence or absence of the organisms at the mat surface.

In this paper we describe the diel migration patterns, or lack thereof, of a few predominant microbial species in a mat from a hypersaline pond. We quantified the migration parameters by using a new technique which involved repeated coring of experimental mats with glass capillary tubes (to obtain minicores). The minicores allowed us to microscopically quantify both the depths of specific layers of microorganisms (by using color and visible light and/or infrared fluorescence) and the relative distributions of identifiable microbial forms within the mat. We also measured some physicochemical parameters, experimentally modified those parameters, and performed physiological experiments with field material in an attempt to

\* Corresponding author. Mailing address: Max Planck Institute for Marine Microbiology, Fahrenheitstrasse 1, 28359 Bremen, Germany. Phone: 421 2208-165. Fax: 421-2208-130. Electronic mail address: ferran@postgate.mpi-mm.uni-bremen.de.

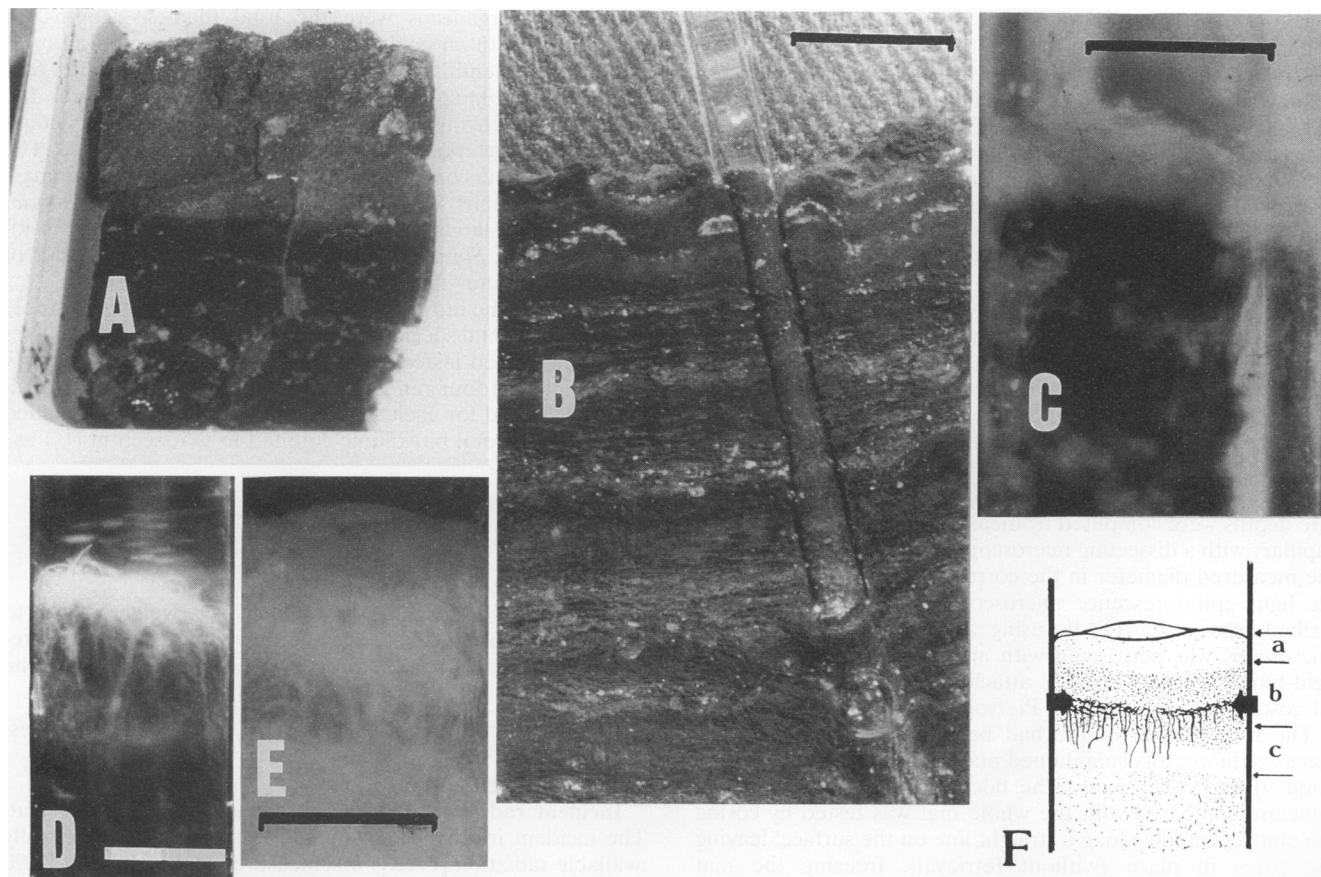


FIG. 1. Microbial mat and minicore technique. (A) Midday appearance of an excised piece of pond 9 microbial mat, showing changes in surface appearance due to cyanobacterial migration. In this case, the bottom one-half of the mat had been shaded with aluminum foil, whereas the top half had been exposed to full sunshine. (B) Minicore sampling maintained faithfully the vertical structure of a well-laminated, highly organic microbial mat. The minicore was removed, the rest of the mat was frozen and cut vertically along the coring line while it was still hard, and the minicore was reinserted into the original orifice. The continuity of the bands and layers is obvious. Bar = 0.5 cm. (C) Photomicrograph of a pond 9 mat minicore taken during the day, showing the top yellow layer, the dark blue-green layer beneath the yellow layer, and a band of *Beggiatoa* sp. The olive green layer could not be distinguished in black and white photographs. Bar = 1 mm. (D) Photomicrograph of a pond 9 mat minicore taken during the night, showing the absence of a top yellow layer and two white bands of *Beggiatoa* sp., one at some depth and one at the top of the mat. Illumination of the core from the top enhanced the appearance of the highly scattering *Beggiatoa* filaments at the top. The combing effect of the minicore on the large *Beggiatoa* filaments at the top can also be observed. Bar = 1 mm. (E) Red epifluorescence photomicrograph of a pond 9 mat minicore taken during the day. The faintly red fluorescent layer at the top corresponds to the yellow layer, and the highly fluorescent layer beneath it corresponds to the blue-green layer. The olive green layer could be correlated with an infrared-fluorescing band when infrared fluorescence microscopy was used (data not shown). Bar = 1 mm. (F) Interpretation of the information obtained in photographs such as those shown in panels C through E for quantification of the bands and layers in a minicore. a, yellow layer; b, blue-green layer; c, olive green layer; thick arrows, *Beggiatoa* band.

relate the pattern and extent of migration to probable environmental cues and to the optimal microenvironment for growth and survival of the organisms.

#### MATERIALS AND METHODS

**General.** We used a laminated, gelatinous, benthic cyanobacterial mat from a hypersaline pond at Exportadora de Sal, S. A., Guerrero Negro, Baja California Sur, Mexico. Most of this study was done in November 1990, although preliminary observations were made with similar mats in previous years and some additional experiments were done in October 1991 and May 1993. In 1990 the mats were obtained from the southeast corner of pond "Area 9" (salt company designation; referred to below as pond 9) at a depth of 0.5 to 1 m; the salinity at this location was 13.5 to 14% (ca. four times that of seawater).

All of the experiments were done with pieces of excised mat (Fig. 1A), which were transported to a temporary laboratory (ca. 20 km from the site) in a plastic pan or dishes after the excess water was removed. The pan was placed outdoors in a bigger pan so that it was bathed with a larger volume of pond 9 water; this kept the temperature of the mat at moderate levels despite insolation. During the midday hours, freshwater ice cubes were occasionally added to the outer bathing water to bring the temperature and salinity down to acceptable levels (the temperature was never more than 28°C). In this arrangement the surface of the mat was about 5 cm below the surface of the water. All core sampling and microelectrode measurements pertaining to the diel cycle were done with a single 1-dm<sup>2</sup> piece of mat after a 5-h period of acclimation to the new setting. Separate pieces were used for other experimental procedures. Diel samples were obtained over a period of 28 h,

starting at 1530 on 10 November 1990 and ending at 1930 on 11 November 1990.

**Minicores.** Cores were taken with glass capillary tubes (outer diameter, 1.5 to 1.8 mm; length, 100 mm; type Kimax-51) that were open at both ends. The capillaries were washed in a 1% Triton X-100 solution immediately before use. Three or four minicores were taken at each sample time, and these minicores were immediately examined with a dissecting microscope. Approximately one-third of all cores attempted were discarded because of poor condition (split, slanted, or too short). The accepted cores were inoculated with a small volume of formaldehyde (15%, wt/vol) by syringe through the top and were immediately sealed top and bottom with plugs of clay, labeled, and stored in the dark at 4°C. Projections of photomicrographic slides of the cores were used to measure the relative depths of the layers, which were distinguished by color (Fig. 1C). Identification and resolution of overlapping bands were aided by examining whole cores by epifluorescence microscopy at red and infrared wavelengths (Fig. 1E). Absolute depths were computed by measuring the diameter of each capillary with a dissecting microscope and relating this value to the measured diameter in the corresponding projection. Visible light epifluorescence microscopy was performed as described previously (11) by using an  $\times 4$  objective. Infrared microscopy was performed with an infrared-sensitive, visible light-blocked video camera attached to an epifluorescence microscope, as described by Pierson and Howard (29).

The minicore technique had been tested previously with pieces of laboratory-maintained mats (some pieces were from pond 9) and other mats. The fidelity of the layering in the minicore compared with the whole mat was tested by coring the mat repeatedly along a straight line on the surface, leaving the cores in place (without retrieval), freezing the mat ( $-20^{\circ}\text{C}$ ), and cutting it while it was frozen along the coring line with a razor blade. The minicores were then retrieved. After each core was reinserted into its original orifice and the positions of the mat surfaces within and outside the minicore were matched, the continuity of the identifiable layers was determined with a dissecting microscope (Fig. 1B). In the study mats, the top 2 to 3 mm of structure was maintained without significant deviations, although some expansion of layers occurred at the lower ends of the cores. In addition, problems were occasionally encountered in the field with some of the larger filamentous *Beggiatoa* spp. since the capillary tubes seemed to pull the *Beggiatoa* filaments out of the mat matrix and drag them along the core-glass interface, giving the appearance of a comb-shaped band that, presumably, was wider than the band in the undisturbed mat (Fig. 1D). Combing was taken into account in the quantification study; zones in which most filaments were vertically aligned were considered sampling artifacts.

**Microscopy and counts.** The capillary tubes were broken so that the upper opening of each tube was close to the core surface, and the cores were pushed from below with a toothpick. Each emerging core was laid onto a glass slide, and several drops of warm, liquid agar (1.5%, wt/wt) were poured over it to fix it and to prevent desiccation. Each core was cut with a razor blade into four serial sections (each approximately 0.4 mm thick), starting from the top; the remainder of the core was discarded. The sections were placed on glass slides in 1 drop of water, and each section was chopped and stirred to achieve an even distribution; then each preparation was mounted under a petroleum jelly-sealed coverslip. Counts were determined with a phase-contrast microscope on four randomly chosen fields. The values used for the unicellular organisms were the numbers of cells. The values used for the

filamentous organisms were the total filament lengths, as determined with an ocular micrometer. We counted all morphologically identifiable species except the purple sulfur bacterium *Thiocapsa* sp., which appeared only in some cores and had a very patchy distribution. Smaller, unidentifiable bacteria (bacilli, flexibacteria, and spirochetes) were also ignored. The final cell numbers or total lengths were converted into biomass (biovolume) units with stereometric formulae. *Oscillatoria*, *Beggiatoa*, and larger *Chloroflexus*-like trichomes were considered cylinders. *Spirulina* spp. cells were considered stacks of toroids (doughnut-shaped structures).

Because of the intricate nature of the mat, it was not feasible to determine total species-specific biomass. Relative biomasses were determined instead. For example, in section  $j$ , species  $k$  was counted in four randomly chosen fields. The total biovolumes measured for each species in a section ( $v_{jk}$ ) were added to obtain the total biovolume counted in that section ( $V_j$ ) as

$$V_j = \sum_{k=1}^{k=n} v_{jk}$$

The  $k$ -specific counts for each section were weighted by  $V_j$  to obtain a weighted species-specific biovolume ( $v_{j,k}^*$ ). The resulting biovolumes were finally expressed as percentages of the

total biovolume for that species ( $\sum_{j=1}^{j=4} v_{j,k}^*$ ) to obtain a species-specific relative depth distribution.

**Incident radiation and radiative transfer within the mat.** The incident irradiance at 400 to 700 nm (photosynthetically available radiation [PAR]) was measured with a model LI-190 quantum sensor. This sensor (flat, cosine response) was placed ca. 10 m from the main work area. Measurements (averages for 10-min intervals) were obtained for the duration of the experiments and were stored in a LI-COR model LI1000 data logger. Radiant energy penetration was measured in the laboratory with a core (diameter, 1 cm) that had been fixed in 5% formaldehyde and kept in the dark and cold; we used an optic fiber (diameter, 1 mm) with a blunt tip attached to a LI-COR model 1800 spectroradiometer as described by Pierson et al. (31). The tip was introduced into the mat core from below and was moved upward through it in 0.1- to 0.3-mm intervals with a micromanipulator. Spectra were recorded at each depth in 2-nm wavelength intervals from 400 to 1,100 nm. We used a 45-W halogen lamp (General Electric) as the light source over the mat. All of the data presented below were normalized to the light intensity measured at the surface of the mat. Mathematically smoothed second derivatives of spectral transmittance were used to better identify the main photopigments present at different depths.

**Oxygen concentration profiles.** Oxygen concentrations within the mat were measured with microelectrodes (33, 34). The microelectrodes used were of the Clark type with built-in reference and a tip diameter of ca. 50  $\mu\text{m}$  (Diamond General Corp., Ann Arbor, Mich.). Each electrode was attached to a micromanipulator and was positioned by using a telescopic viewer so that the tip was touching the surface of the mat. After this, the positions within the mat were read on the micromanipulator scale. The electrodes were calibrated by taking readings in aerated pond water ( $\text{O}_2$ -air saturation) and deep ( $>3$  mm) within the mat (zero). The responses were determined with a Diamond General model 1201 chemical microsensor analyzer set at a cathode polarization value of  $-0.75$  V.

TABLE 1. Principal bacterial taxa studied, some of their relevant characteristics, and their relative contributions to total biovolume in the top ca. 1.6 mm of mat

Taxon <sup>a</sup>	Cell diam ( $\mu\text{m}$ )	Major pigments	Morphology	% Of total measured biovolume (SD)	Gliding speed ( $\mu\text{m s}^{-1}$ ) <sup>b</sup>
Cyanobacteria					
<i>Cyanothece</i> sp. ( <i>Aphanothece halophitica</i> )	4.3	Chl <i>a</i> , phycocyanin	Unicellular	34.6 (12.7)	
<i>Oscillatoria</i> sp.	3.5–3.9	Chl <i>a</i> , phycocyanin	Filamentous	14.9 (5.8)	0.98–1.02
<i>S. subsalsa</i>	2.1–2.3 <sup>c</sup>	Chl <i>a</i> , phycocyanin	Coiled filaments	15.0 (7.7)	0.6–0.7
<i>S. labyrinthiformis</i>	1.2 <sup>d</sup>	Chl <i>a</i> , phycocyanin	Coiled filaments	5.7 (4.4)	0.26–0.30
Anoxyphotobacterium ( <i>Chloroflexus</i> -like sp. [“ <i>Oscillochloris</i> ” sp.]	1.3–1.4	BChl <i>c</i> , BChl <i>a</i>	Filamentous	7.3 (2.9)	
Colorless sulfur bacterium ( <i>Beggiatoa</i> sp.)	7–8		Filamentous	21.9 (11.1)	0.98–2.65

<sup>a</sup> Generic assignments according to reference 39a.<sup>b</sup> See text for discussion of gliding speed.<sup>c</sup> Coil diameter, 5.3 to 5.6  $\mu\text{m}$ .<sup>d</sup> Coil diameter, 2.5 to 2.8  $\mu\text{m}$ .

**Physiological experiments and determinations.** Gliding motility rates were measured directly with a microscope with freshly collected materials. The means for seven or eight filaments in two different preparations are given below. Photosynthesis was measured by the  $\text{NaH}^{14}\text{CO}_3$  method with a suspended mixture containing mainly *Oscillatoria* sp. and *Spirulina subsalsa*. This suspension was purified from the mat community according to the clumping behavior of gliding filamentous cyanobacteria (3, 4). Morning surface samples were dispersed with a glass tissue grinder in pond 9 water cleared by filtration through glass fiber filters (Whatman type GF/F) and were allowed to stand for ca. 5 min until they formed a visible clump of trichomes. The water was poured out, and new water was added. This procedure was repeated three times, and the final suspension was used for experiments. An aliquot of the suspension was fixed with formaldehyde, and later the following species composition (based on biovolume) was determined: *Oscillatoria* sp., 53.18%; *S. subsalsa*, 31.50%; *Cyanothece* sp., 6.50%; *Beggiatoa* sp., 7.14%; *Chloroflexus* type or “*Oscillochloris*” sp., 0.61%. The photoautotrophic incorporation results were therefore assigned to a mixture of *Oscillatoria* sp. and *S. subsalsa*. The final suspension was subdivided into aliquots and dispensed into sterile glass tubes with rubber stoppers. One  $^{14}\text{C}$  experiment was designed to test the ability of the motile cyanobacteria to withstand soluble sulfide and to perform facultative anoxygenic photosynthesis with sulfide as an electron donor. The parameters measured included the “control” rate of oxygenic photosynthesis, the rate of photosynthesis obtained with the photosystem II inhibitor 3-(3,4-dichlorophenyl)-1,1-dimethylurea (DCMU; final concentration, 7  $\mu\text{M}$ ), the rate of photosynthesis in the presence of 0.6 mM sulfide, the rate of photosynthesis in the presence of DCMU and sulfide, and the corresponding values for dark controls for all preparations. A more detailed description has been published previously (10). Triplicate samples were incubated outdoors for 30 min under ca. 200  $\mu\text{mol}$  of photons  $\text{m}^{-2} \text{s}^{-1}$ . In a second experiment we tried to establish a curve for relative photosynthesis versus light intensity and to determine the light intensity that resulted in onset of photoinhibition. Triplicate samples were incubated for 1 h. Different levels of irradiance were obtained by placing sample tubes under layers of fiberglass mesh screen. A final radiotracer activity of 0.12  $\mu\text{Ci ml}^{-1}$  was used, and incorporation was stopped by adding formalin (final concentration, 5%, vol/vol). Samples were processed as described previously (10). A lack of knowledge concerning the equilibrium constants of the bicarbonate system in highly saline waters (15) prevented calculation of the

total amount of carbon fixed. The final data are expressed below in disintegrations per minute.

The specific chlorophyll *a* (Chl *a*) contents were determined spectrophotometrically after extraction in methanol of samples whose biomasses had been determined gravimetrically (dry weight) as described previously (11, 12).

## RESULTS

**Structure of the microbial mat.** The mat harbored a variety of morphologically recognizable microorganisms embedded in a gelatinous matrix. It changed in surface color from a very dark green (at night) to a greenish yellow (during the day) because of the presence or absence of the bulk of the migrating cyanobacteria (Fig. 1A). The mat was organized into visibly distinct layers that could be assigned to specific groups of microorganisms (Fig. 1B and C), including a dark blue-green layer of pigment-rich cyanobacteria, a white layer containing sulfide-oxidizing *Beggiatoa* sp., and a deeper olive green layer with bacteriochlorophyll *c* (BChl *c*)-containing filamentous photosynthetic bacteria (i.e., “*Oscillochloris*” sp. or *Chloroflexus*-like organisms). The average species composition of the upper ca. 1.6 mm (expressed as percentages of the total biovolume) is shown in Table 1, together with some relevant characteristics of the main species involved. The sequence of the layers in the community was dynamic, and there were conspicuous differences between daytime and nighttime at different depths. During the night, the blue-green (strongly red-fluorescing) layer spanned the distance between the surface and a depth of ca. 0.7 mm, and the olive green (infrared-fluorescing) layer was immediately below this layer. Two distinct layers containing *Beggiatoa* sp. were visible, one at the surface of the mat (at night) and one between the blue-green and olive green layers (at all times). At midday, the blue-green layer was down at a depth of 0.4 to 0.7 mm, and a new, yellow (dimly red-fluorescing) layer was present at depths between 0 and 0.4 mm. The olive green layer remained at the same position at a depth of more than ca. 1 mm.

**Layer dynamics within the mat community.** Some migration patterns within the mat were revealed by the minicore data (Fig. 2). The blue-green, strongly red-fluorescing layer underwent changes in the position of its upper boundary, which was usually sharply demarcated. This boundary went down during the daytime and reached a maximum measured mean depth of 0.5 mm, leaving behind a yellow, faintly red-fluorescing, more translucent layer (Fig. 2B). The depth of the upper boundary of the blue-green layer was inversely correlated with the

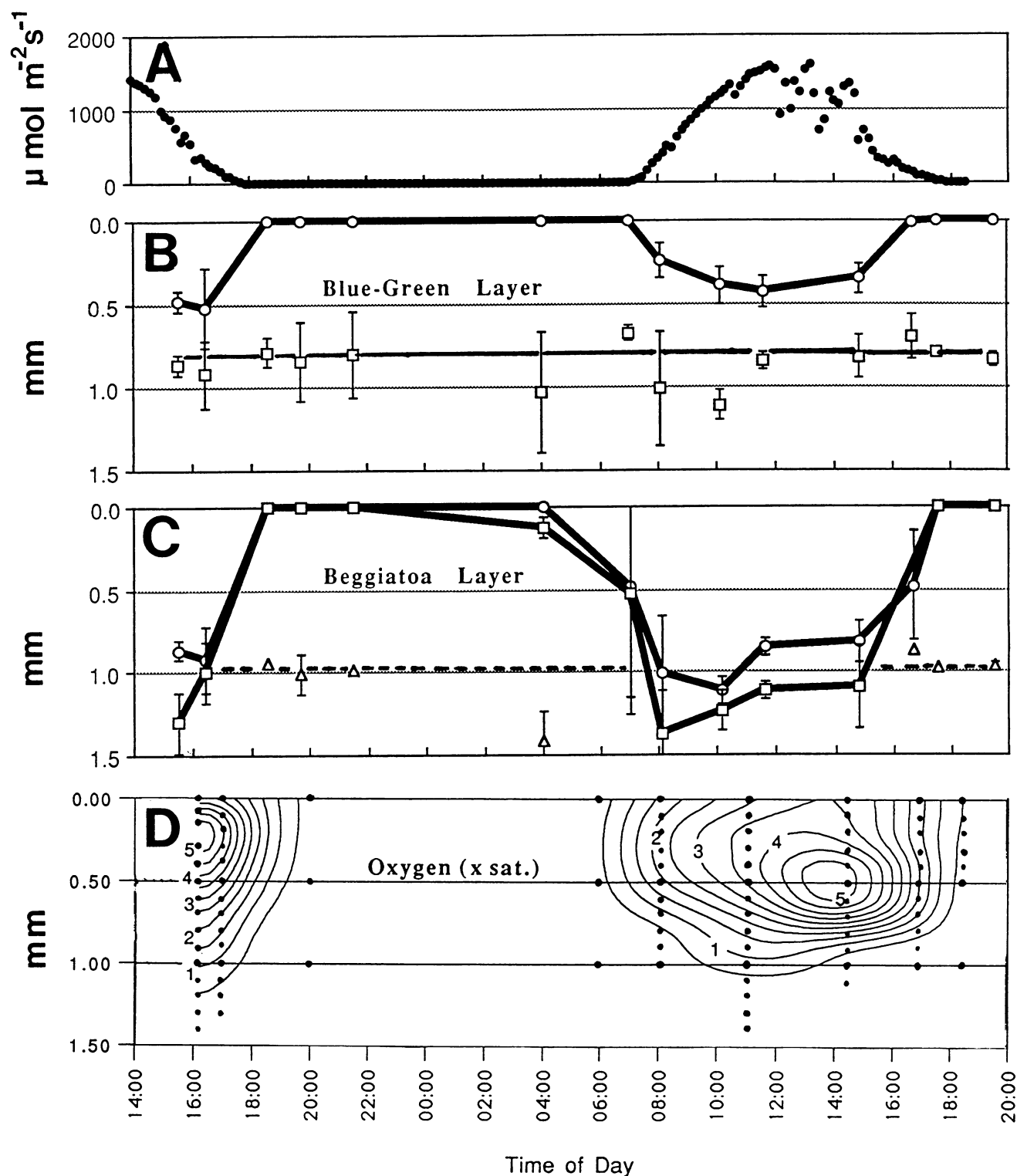


FIG. 2. Dynamics of light regime, microbial layer depth, and oxygen concentration during a diel cycle in the 1991 mat. (A) Incident irradiance (wavelengths, 400 to 700 nm). The values are integrated over 10-min intervals. (B) Mean depths ( $n = 3$ ) of the upper (○) and lower (□) boundaries of the blue-green layer obtained from minicores. The bars indicate 2 standard deviations. (C) Mean depths ( $n = 3$ ) of the *Beggiatoa* layers obtained from minicores. Symbols: ○ migrating *Beggiatoa* upper boundary; □, migrating *Beggiatoa* lower boundary; Δ, nonmigrating *Beggiatoa* sp. The bars indicate 2 standard deviations. (D) Isopleths of oxygen concentration within the mat obtained from microelectrode measurements (the units are times saturation). The dots are the actual data points, and the lines are the result of mathematical interpolation.

incident irradiance outside the mat (Fig. 2A). The values for the lower boundary of the blue-green layer exhibited greater variance within replicates, and a migration pattern was not obvious, which we interpreted as a reflection of a nonmigrating lower boundary.

The *Beggiatoa* layer was, in general, quite thin (ca. 0.1 mm) and, unlike the blue-green layer, moved as a distinct band (Fig. 2C). Surprisingly, a band of *Beggiatoa* sp. occurred at some depth during the night, when another band of *Beggiatoa* sp. was at the surface of the mat. During the daytime, only one band was visible, and it was at some depth, just below or within the lower boundary of the blue-green layer. Our results indicated that the single daytime *Beggiatoa* band split at night, with one part migrating upward to the mat surface (migrating *Beggiatoa* band) and a second part staying behind (nonmigrating *Beggiatoa* band). Microscopically, the two subpopulations were indistinguishable, in both trichome and cell size, and both contained abundant sulfur granules at all times. However, during subsequent investigations in 1991 in which similar mats were used, a nonmigrating *Beggiatoa* band was not observed.

Within replicate cores, the variation in the measured depth and thickness of the olive-green, infrared-fluorescing layer was greater the variation observed with other layers, although for each individual core, the upper boundary of this layer was below the blue-green layer. The mean depth of the upper boundary was 0.9 mm, and the mean depth of the lower boundary was 1.7 mm. For this layer, there was neither a conspicuous diel change in depth nor changes in position relative to the other layers.

The mat was subject to marked, at times very rapid, changes in  $O_2$  concentration, which ranged from 5.5 times saturation in the afternoon to complete anoxia shortly after dusk and during the night (Fig. 2D). Sulfide accumulated during the night and diffused from the mat into the overlying water. Sulfide was detected with methylene blue reagent (6), but was not quantified. From the oxygen profiles shown in Fig. 2, it is evident that the maximum oxygen concentration within the mats followed the diel behavior of the upper boundary of the blue-green layer. The migrating *Beggiatoa* band closely followed the isopleth of oxygen subsaturation.

**Specific depth distributions and migratory behavior.** The relative levels of the major quantifiable mat species are shown in Fig. 3. These levels are expressed as the percentage of the total weighted biovolume determined for each species that was found in four sequential sections. Data for two representative times, one at night (0400) and one during the day (1530), are given. The relative biomass distribution data are in agreement with the general patterns observed with the minicores. In the case of *Beggiatoa* sp., there were virtually no filaments in the upper 0.8 mm of the mat during the day, and two distinct populations were found at night. On the basis of the distribution data, however, we discovered that most of the *Beggiatoa* biomass came from the nonmigrating *Beggiatoa* fraction. Another clear pattern of distribution was the *Chloroflexus*-like-*Oscillochloris* pattern; most of the population was found at depths greater than 1.2 mm both during the day and night. For *Cyanothece* sp., most of the cells were found in the top 0.8 mm of mat, even though a significant fraction (20 to 30%) was found at greater depths. The distribution of the small *Spirulina* species (*Spirulina labyrinthiformis*) seemed to be skewed toward the mat surface, at least in the daytime core data. Some differences were found between the daytime and nighttime cores with this organism, but the possibility that there was a slight nighttime downward migration suggested by these data must be regarded with caution, since *S. labyrinthiformis* was present in disjunct patches, not only vertically but also hori-

zonally. The two filamentous cyanobacteria that were probably responsible for the migration observed in the minicores are *Oscillatoria* sp. and the large *Spirulina* species (*S. subsalsa*), since these organisms constituted a fraction of the total biomass (Table 1) large enough to account for the changes in the appearance of the mat. These two species were present in significant amounts throughout the mat. Thus, the olive green layer, visually assigned to *Oscillochloris* sp., was far from specific and harbored a high percentage of cyanobacteria as well. A pattern of migration between day and night was clearer for *Oscillatoria* sp. than for *S. subsalsa*; however, the rather large standard deviations obtained with replicate cores made it difficult to extract definitive conclusions. Since the cyanobacterial migration occurred within the first 1 mm of the mat, we performed statistical calculations with the data obtained from the top ca. 0.8 mm in order to determine which species were responsible for the blue-green migration. In this case the data represented the percentage of each species found either between 0 and 0.4 mm (up) or between 0.4 and 0.8 mm (down), compared with the total biomass for that species in the interval

$$j=2$$

from 0 to 0.8 mm ( $\sum_{j=1}^2 v^*_{jk}$ ), and we included data obtained

$$j=1$$

from cores taken at other times during the diel cycle. Figure 4 shows the diel variations in the relative positions of *Oscillatoria* sp. and *S. subsalsa*. For statistical analysis, the percentages were pooled, as described above, into daytime and nighttime groups. The percentage data were transformed to the square root of the arcsine (angular transformation), which is typical for proportions (39). One-way analyses of variance were performed to compare the variation in the percentages of biomass that were up within and between the daytime and nighttime groups. The comparison of daytime data and nighttime data resulted in a highly significant difference ( $P = 0.0003$ ; F test) only for *Oscillatoria* sp. The *S. subsalsa* data were significantly different only after one outlier datum point was removed ( $P = 0.014$  without the outlier;  $P = 0.127$  with the outlier). The *Cyanothece* sp. ( $P = 0.223$ ) and *S. labyrinthiformis* ( $P = 0.804$ ) differences were not significant. It is clear that *Oscillatoria* sp. was responsible for at least part of the migration of the blue-green layer, and it is probable that *S. subsalsa* also contributed to this migration. In previous and subsequent years (1988, 1991, 1993), *S. subsalsa* was the dominant cyanobacterium in the mats, and cyanobacterial diel vertical migration was also documented.

#### Radiative transfer within the mat and pigment analysis.

Radiative transfer within the mat was expressed as the fractional spectral transmittance (by normalizing the spectrum at a certain depth to the spectrum at the surface). The core which we analyzed was taken and preserved at 1000. The results of the second derivative analysis are shown in Fig. 5. Overall, the spectra revealed the opacity of the microbial assemblage: visible light (400 to 700 nm) was extinguished below or around the 1% level at a depth of ca. 0.5 mm. According to physiological data for cultures (2) and measurements obtained from cyanobacterial mats (16, 19, 21, 32), the effective euphotic zone for cyanobacteria could not have reached much deeper than this (at most 0.75 mm), assuming that the layer was static. In the infrared portion of the spectrum, however, there was some available radiation (more than 1% of the surface value) even at a depth of 1.0 mm.

The transmittance characteristics of the top yellow layer were important because they were used to estimate the shielding gained by the migrating blue-green components. As determined by observations of minicores, only the spectrum of the

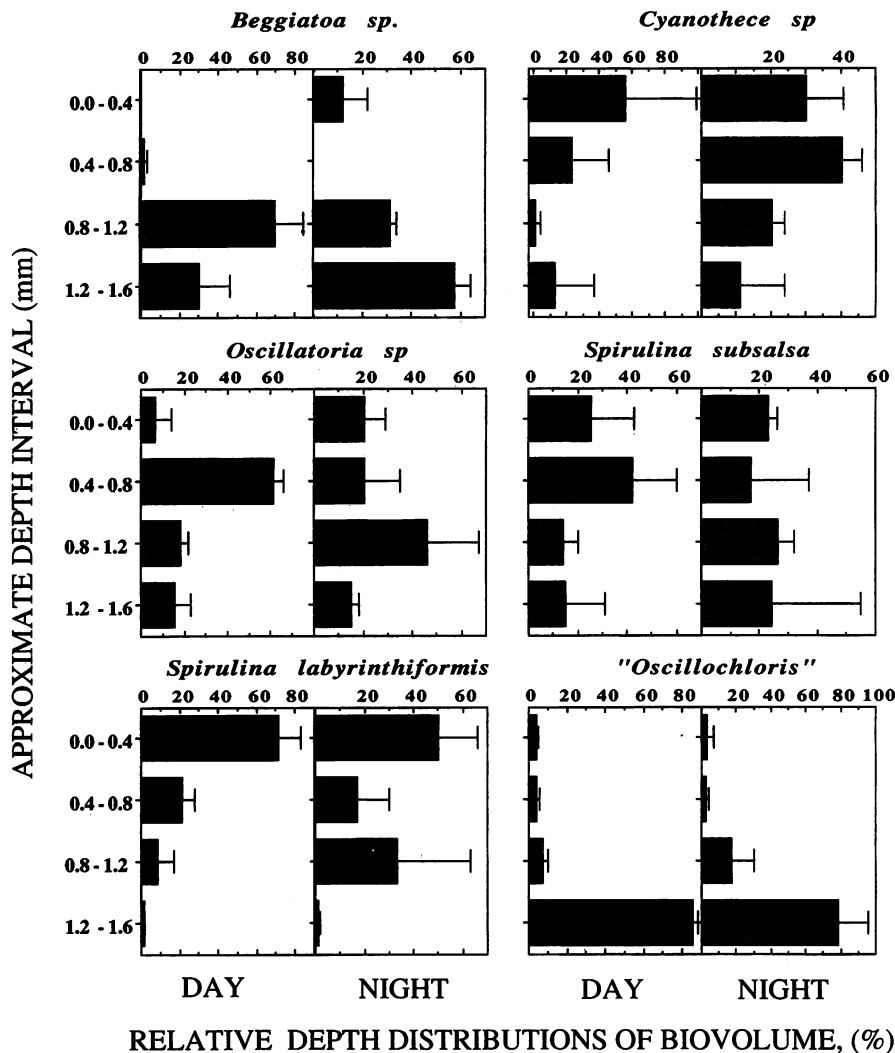


FIG. 3. Relative biovolume depth distributions for the major morphotypes in the mat obtained from microscopic counts of minicores. The distributions for each species are shown in two panels; the left panels show the data for samples taken at 1530 in the diel cycle, the right panels show the data for samples taken at 0400. Four serial sections that were ca. 0.4 mm thick were examined per core. Each datum point represents the mean count obtained for three cores taken simultaneously. The bars indicate standard deviations.

mat core used for the light penetration measurements obtained at a depth of 0.1 mm could be confidently assigned to this layer. In the upper layers of the mat (down to a depth of 0.3 mm) we observed strong extinction of the shorter visible light wavelengths (because of carotenoids and the Soret band of Chl *a*). The peaks at 670 to 675 nm (Chl *a*) and at 625 to 630 nm (phycocyanin) were clear; absorption in the infrared portion of the spectrum was weak. This pattern of absorption was attributable to the cyanobacteria and was consistent with previously published spectral data (17, 19, 21, 30, 31). Spectra obtained at depths of 0.75 mm or more exhibited, in addition to the features described above, absorption in the infrared region; various peaks were observed. These absorption peaks were attributed to BChls, including BChl *a* (790 to 810 and 830 to 920 nm), BChl *c* (740 to 755 nm), and, possibly, BChl *d* (725 to 745 nm). A small peak in the green region was tentatively attributed to cyanobacterial phycoerythrin. The presence of BChl *c* is typical of the known *Chloroflexus* and "*Oscillochloris*" species.

Careful sampling of the *Oscillatoria*-*S. subsalsa* trichomes from the blue-green layer (four samples) yielded Chl *a*-specific content values between 2.3 and 3.9% of the dry weight. In two samples, the yellow top layer containing mostly *Cyanothece* sp. yielded values of 0.3 and 0.35% of the dry weight. A patch containing a yellowish green population of mostly *S. labyrinthiformis*, which exhibited a shallow migratory pattern, gave a value of 1.4% of the dry weight. The presence of both BChl *c* and BChl *a* at some depth was confirmed in the cores used for the diel cycle by using *in vivo* absorption spectroscopy and methanol extracts of core slices (data not shown).

**Light manipulation.** In order to determine whether light was involved directly or indirectly in migration, the light intensity was decreased and light was eliminated by using multiple layers of window screen (untinted fiberglass) and black cloth, respectively. Cores taken before and after the treatments were compared.

One set of samples was shaded at dawn (both *Beggiatoa* sp. and migrating cyanobacteria were at the mat surface) and was

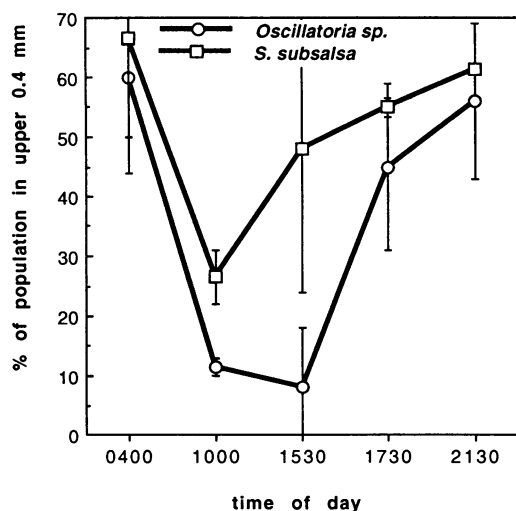


FIG. 4. Relative distribution of biovolume within the top 0.8 mm of mat for both *S. subsalsa* and *Oscillatoria* sp. versus time. A statistical analysis was performed with this type of data for all cyanobacterial species counted (not all are shown on the graph; see text) to determine which organisms were responsible for the migration of the blue-green layer (Fig. 2B).

analyzed near midday both by the minicore technique (species) and by determining  $O_2$  concentrations (Fig. 6). Downward migration of the blue-green layer did not occur in the dark or when only 10% of the incident irradiance was available. When 56% of the incident irradiance was available, migration occurred, but the organisms migrated to a shallower depth than they did in the control (full light intensity). The oxic zone was deepest in the control and was progressively shallower and less pronounced when 56 and 10% of the incident irradiance were available. The darkened mat remained anoxic throughout. *Beggiatoa* sp. was at a depth close to the oxic-anoxic interface in all of the treatments except the dark treatment, in which a band was not present and the trichomes were dispersed.

In addition, shading or darkening of midday, sun-exposed mats from which surface migrating populations had ostensibly disappeared resulted in the ascent of the upper boundary of the blue-green layer and some *Beggiatoa* sp. cells to the mat surface within 1.5 h. In every case the movement to the surface was more rapid when low light intensity was used than when complete darkness was used (data not shown).

**Photosynthetic capacities of the migrating cyanobacteria.** The radiolabeled bicarbonate photoincorporation experiments revealed that the mixture of *Oscillatoria* sp. (53%) and *S. subsalsa* (31%) reached photosynthetic saturation at a fluence rate of about  $200 \mu\text{mol m}^{-2} \text{s}^{-1}$  (400 to 700 nm) and exhibited photoinhibition at fluence rates greater than  $400 \mu\text{mol m}^{-2} \text{s}^{-1}$  (Fig. 7). Photoincorporation of radiolabel (light minus dark) in the suspension was efficiently prevented by the addition of DCMU (a photosystem II inhibitor), but addition of 0.6 mM sulfide in the presence of DCMU resulted in substantial incorporation (Fig. 8). This is evidence that sulfide-driven, photosystem I-mediated anoxygenic photosynthesis occurred. Since the level of  $^{14}\text{C}$  photoincorporation in the presence of sulfide alone was not significantly higher than the level of  $^{14}\text{C}$  photoincorporation observed in the presence of sulfide plus DCMU, we inferred that sulfide effectively inhibited photosystem II activity (10). Therefore, it is probable that

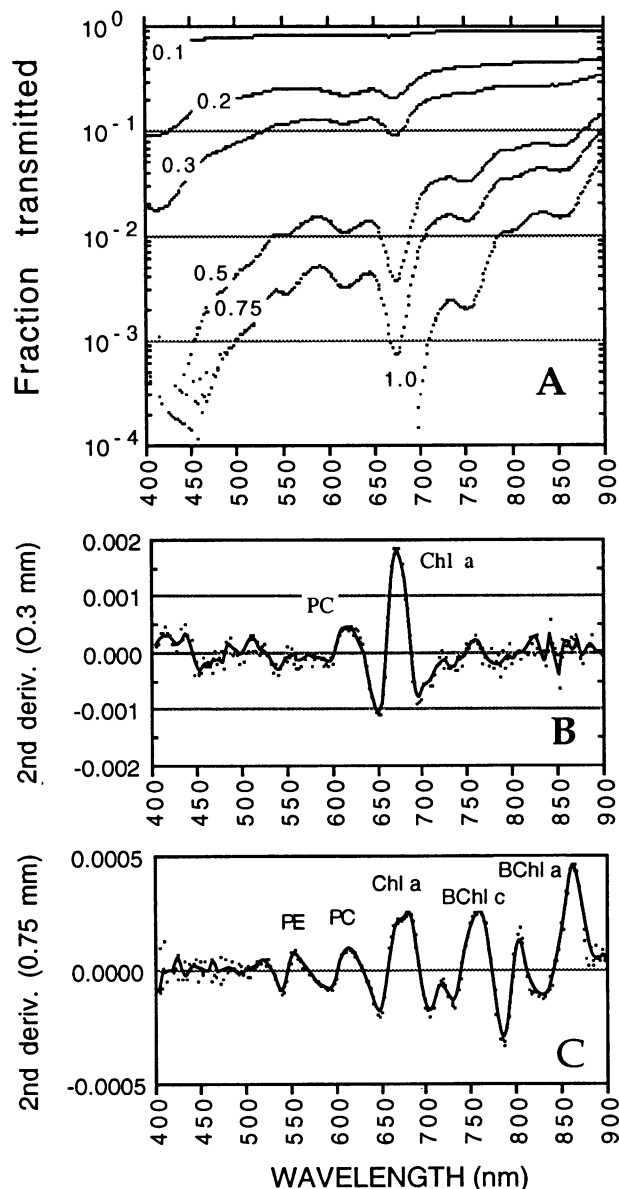


FIG. 5. Fractional spectral transmittance with depth in the microbial mat and derivative analysis of the data for a midmorning mat core. (A) Fractional spectral transmittance. The depth in millimeters is indicated for each spectrum. Data were expressed as the ratio of the measured spectral light intensity to the light intensity at the surface of the mat. (B) Second derivative plot of the fractional transmittance spectrum at a depth of 0.3 mm. Peaks for the major pigments responsible for absorption at the longer visible light wavelengths (Chl *a* and phycocyanin) are conspicuous. At shorter wavelengths measurements were less accurate because of the lower output of the light source used. (C) Same panel as B, except that the data were obtained at 0.75 mm. Individual peaks were assigned to plausible compounds on the basis of peak absorption. PE, phycoerythrin; PC, phycocyanin.

photosynthesis changed from an oxygenic reaction to an anoxygenic reaction when sufficient sulfide was encountered.

## DISCUSSION

The general pattern of diel migration for both cyanobacteria and *Beggiatoa* sp. in the mat which we examined consisted of a

daytime descent and a nighttime ascent. This pattern is commonly encountered (3, 5, 40), although a more complicated pattern that includes a second, nighttime descent has been described (36). The migration occurred against a background of static species; the cyanobacteria, *Cyanothece* sp. and *S. labyrinthiformis*, and the filamentous anoxygenic *Chloroflexus*-like bacteria did not migrate, even though some form of gliding motility is known for all of these organisms. On one occasion, however, slow migratory activity was detected in a patch that had a population dominated by *S. labyrinthiformis* (data not shown). *S. labyrinthiformis* apparently exhibits short vertical migration that could not be resolved in the main mat which we studied.

**Migration of *Beggiatoa* sp.** Colorless sulfur bacteria that oxidize hydrogen sulfide with molecular oxygen are typically gradient organisms that inhabit the interfaces of oxygen and sulfide in nature (18). These bacteria are known to follow moving interfaces by means of active, fast, gliding or swimming motility, often giving rise to spatially defined bacterial plates (9, 24, 26). In microbial mats, this often translates into populations that move into the mat during the daytime and return to the top of the mat at night (25). In this study, as predicted, during the daytime and during experimental manipulations, the position of the *Beggiatoa* sp. band was determined by the oxic-anoxic interface (Fig. 2C). However, two distinct subpopulations were repeatedly distinguished during the night, a migrating subpopulation that rose to the surface and a nonmigrating population that stayed at some depth (Fig. 1C and 3). The fact that during the following day only one band of migrating *Beggiatoa* sp. was seen when the oxic-anoxic interface penetrated the mat suggests that the two subpopulations fused into one population that followed the interface closely. The speed of ascent of the oxic-anoxic interface calculated from the oxygen profiles at dusk was at least  $0.6 \text{ mm h}^{-1}$ . It is conceivable that a certain proportion of the population could not keep up with the moving interface, since the gliding speeds measured for *Beggiatoa* sp. ( $0.3$  and  $0.9 \text{ mm h}^{-1}$ ) (Table 1) are both greater and less than the speed of movement of the interface. This may not be a general phenomenon; in a variety of mats in 1991, which were also studied by using minicores, only a migrating *Beggiatoa* band was observed.

**Cyanobacterial migration.** *Oscillatoria* sp. and *S. subsalsa* migrated downward into the mat in a pattern that was closely correlated with the level of incident irradiance over the surface. The migration was conspicuous at midmorning, and the organisms reached their maximal depths in the afternoon (average depth,  $0.5 \text{ mm}$ ). Near dusk, very fast upward movements occurred. Both *Oscillatoria* sp. and *S. subsalsa* are relatively fast gliders. The gliding speeds measured for both species could easily account for the distance covered in the time scales observed with the migration phenomenon. The maximum advance speeds of the blue-green layer, when it was ascending at dusk, were about  $0.2 \text{ mm h}^{-1}$ . Judging from the trichome gliding speeds which were measured (Table 1), *Oscillatoria* sp. could potentially cover  $0.39 \text{ mm h}^{-1}$  and *S. subsalsa* could cover  $0.29 \text{ mm h}^{-1}$ . *S. labyrinthiformis*, however, could cover only  $0.08 \text{ mm h}^{-1}$ , and *Cyanothece* sp. was practically nonmotile over the time scales used, even though very slow gliding motility has been observed with this unicellular cyanobacterium (38). This finding is consistent with the results obtained in the biomass analysis (Fig. 3 and 4), which identified *Oscillatoria* sp. and *S. subsalsa* as the most probable migrating components.

Cyanobacterial downward migration into mats is thought to be a mechanism by which organisms avoid exposure to high levels of irradiance during the day and therefore avoid photo-

inhibition of photosynthesis and other photodamage (3, 5, 28, 40). It has been suggested that such tactic mechanisms permit cyanobacteria to retain high levels of light-harvesting pigment (i. e., chlorophyll and phycobilins) without the likelihood of photodamage by absorption of excess photons (5). In this study both *Oscillatoria* sp. and *S. subsalsa* were profusely pigmented (typical for shade-acclimated cells), whereas *Cyanothece* sp. and *S. labyrinthiformis* had low pigment contents (typical for photobleached, sun types). The latter organisms comprised the translucent yellow layer in the daytime top mat. The yellow species were therefore exposed to full sunlight at midday, whereas the migrating species were shaded by the yellow layer. In the mats which we studied, it was very clear that the migrating species had rather high Chl *a* contents (up to 3.9% of the dry weight), whereas the nonmigrating species had Chl *a* contents as low as 0.3% of the dry weight, findings which support the hypothesis described above. The retention of high levels of light-harvesting pigment should allow these cyanobacteria to take advantage of early morning, late afternoon, and overcast conditions when the available photon flux may otherwise be limiting.

It is possible to estimate the irradiance available to migrating cyanobacteria at each time during the diel cycle by using a transmittance value (integrated between 400 and 700 nm, corresponding to the thickness of yellow layer at the time) and the measured surface PAR values. The transmittance value ( $T$ ) is calculated as  $T(t) = (T^*y)^{z(t)}$ , where  $z(t)$  is the mean depth of the migrating cyanobacteria (upper limit) at time  $t$  and  $T^*$  is the PAR mean value of transmittance per unit of depth of the yellow layer, estimated from the spectroradiometric measurement as follows:

$$T^*, (1 \text{ mm}) = \int_{400 \text{ nm}}^{700 \text{ nm}} T(\lambda) \delta\lambda = 0.0491$$

Furthermore, if the available light intensity is known, it is possible to estimate the region on the photosynthesis-versus-irradiance curve (Fig. 7) in which the migrating cyanobacteria should be operating at any given time during the diel cycle. With the exception of the early morning and early evening times, the irradiance values at the upper boundary of the blue-green layer estimated in this way are below or around  $400 \mu\text{mol m}^{-2} \text{ s}^{-1}$ , which is the maximal light intensity for saturation of photosynthesis without significant photoinhibition. The results of these calculations are shown in Fig. 9. It is obvious that, according to these calculations, migration placed all of the migrating cyanobacteria under a light regime in which photoinhibition was effectively avoided, since all of the blue-green layer must have been under light intensities less than  $400 \mu\text{mol m}^{-2} \text{ s}^{-1}$ . A similar calculation for photosynthetic performance was performed for a hypothetical case in which the migrating cyanobacteria had not moved down (Fig. 9) (we assumed that there would be immediate recovery from photoinhibition). According to the results obtained, the cyanobacteria would have been severely photoinhibited during most of the day. These results support the hypothesis that vertical migration is a mechanism by which not only photodamage is avoided but optimal conditions are found. It must be noted that estimates in which PAR integrated irradiance values are used may have inherent errors because the spectral shifts that occur at different depths in the mat are not taken into account (Fig. 5). It is known that longer wavelengths in the visible portion of the spectrum are most efficiently used for photosynthesis in

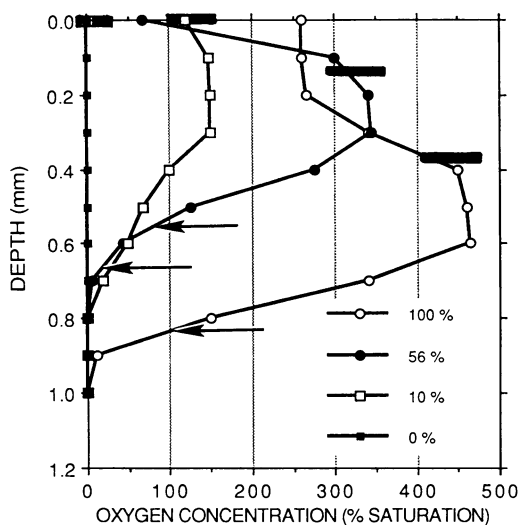


FIG. 6. Midday profiles of oxygen concentration in shaded mats. Pieces of mat were shaded at dawn so that they received 100, 56, 10, and 0% of the incident irradiance. Profiles were measured between 1130 and 1430. The mean depths ( $n = 2$ ) of the upper limit of the blue-green layer (bars) and the *Beggiatoa* layers (arrows) are superimposed on the profiles. Note that downward migration of the blue-green layer occurred only in the mats that received 100 and 56% of the incident irradiance and that the depth-integrated oxygen content in the mat was proportional to the available irradiance.

both cultured (13) and natural populations of mat-forming cyanobacteria (16, 32), and, therefore, these wavelengths can saturate and photoinhibit photosynthesis at lower fluence rates than shorter wavelengths (1). However, blue light and UV radiation at high fluence rates can have severe deleterious effects on photosynthesis and growth as well (12, 14, 41). To account for these effects on the calculations would be extremely difficult, but it is certain that the two types of errors would be in opposite directions, and therefore the use of mean PAR values may be a way to obtain intermediate estimates.

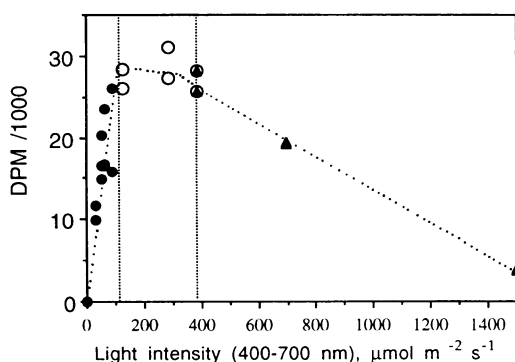


FIG. 7. Relative photosynthesis-versus-irradiance plot for migrating cyanobacteria. Aliquots of a homogenized, enriched suspension containing mainly *Oscillatoria* sp. and *S. subsalsa* were used for  $\text{NaH}^{14}\text{CO}_3$  photoincorporation incubation experiments. Photosynthesis rates were corrected for dark and background uptake and expressed as disintegrations per minute. The following three major domains were distinct: light limitation (up to  $100 \mu\text{mol m}^{-2} \text{s}^{-1}$ ) (●), saturation (100 to  $400 \mu\text{mol m}^{-2} \text{s}^{-1}$ ) (○), and photoinhibition ( $>400 \mu\text{mol m}^{-2} \text{s}^{-1}$ ) (▲).

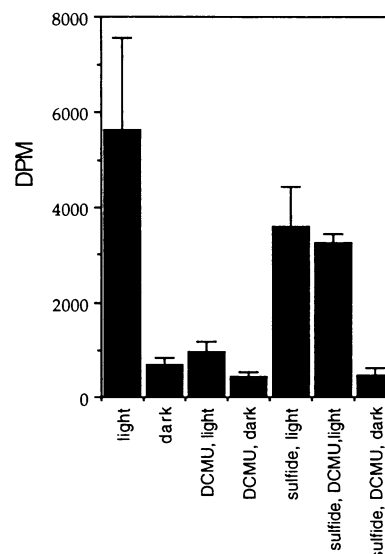


FIG. 8. Incorporation of  $\text{NaH}^{14}\text{CO}_3$  in aliquots of a suspension of enriched *Oscillatoria* sp. and *S. subsalsa* treated to estimate the extent of sulfide toxicity to oxygenic photosynthesis and capacity for anoxygenic photosynthesis. Additions were 0.6 mM sulfide and  $7 \mu\text{M}$  DCMU. Levels of incorporation are expressed in disintegrations per minute. See text for interpretation.

Additional errors may come from our estimates of light intensity. The sensing tip which we used had a wide acceptance angle so that the values measured (radiance with an unspecified solid angle) were only close to the total downwelling irradiance values (17). The measurements obtained with this setup were about 10% lower than the total downwelling irradiance values measured in parallel with an irradiance probe (31). Scalar irradiance, which estimates the light field available coming from all directions, is thought to be best for biological interpretation (21). For strongly absorbing systems, such as the mats which we used, values for scalar irradiance in the visible portion of the spectrum should be at most only 10% higher than downwelling irradiance values (20). The results of a third calculation of the estimated performance of the cyanobacteria, assuming that our irradiance measurements were 20% lower than the scalar irradiance values, are also included in Fig. 9 and show that the main conclusions derived from the physiological estimates were not significantly affected by these sources of error.

Further evidence relating downward migration to negative light responses could be obtained from artificially shading mat pieces; migration did not occur in complete darkness or when 10% of the incident irradiance was available (maximum PAR photon fluence rate, about  $150 \mu\text{mol m}^{-2} \text{s}^{-1}$ ), and the extent of migration decreased when 50% of the incident irradiance was available (maximum value,  $750 \mu\text{mol m}^{-2} \text{s}^{-1}$ ) compared with an unshaded mat. According to the photosynthesis-versus-irradiance curve, cells in the mat that received 10% of the incident light were light limited, but for cells in the mat that received 50% of the incident light, the level of irradiance was great enough to cause photoinhibition had the cells stayed at the top.

A variety of tactic responses could be called upon to explain the overall behavior of the migrating cyanobacteria, including a negative response to sulfide, positive aerotaxis, and a variety of negative and positive light responses. However, responses to

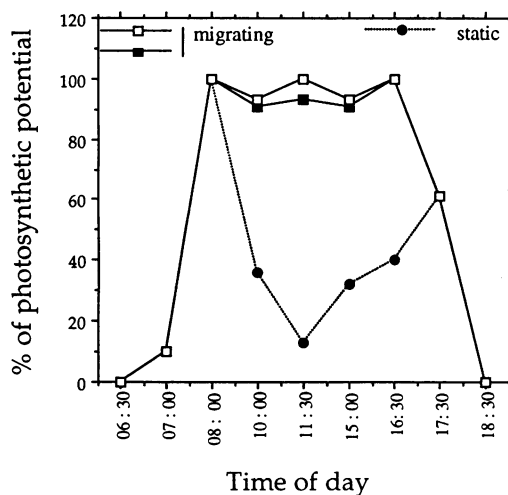


FIG. 9. Estimated photosynthetic capacity (expressed as a percentage of the saturation value) for the upper boundary of the migrating blue-green layer of cyanobacteria during the day. Symbols: □ and ■, estimates accounting for vertical migration; □, values determined by using estimated light fields; ■, values allowing for 20% underestimation of the true light field; ●, calculated photosynthetic rates assuming that migration had not occurred (static). According to our estimates, the migrating cyanobacteria should have been operating at values close to saturation of photosynthesis during most of the day, as a consequence of migration, despite strong insolation around noon.

light alone, such as phobic reactions and/or phototaxis, could explain the descending and ascending behavior of the upper boundary of the blue-green layer (4). However, ascent at dusk occurred not only in the presence of natural waning light intensities but also when the mats were subjected to experimental, sudden, complete darkness, albeit significantly more slowly. This must be explained by chemotactic or chemophobic reactions or perhaps by a random "collection" of trichomes at the surface, which were not forced downward by a light cue. The lack of a diel pattern in the position of the lower boundary of the blue-green layer is somewhat more difficult to explain. Whereas it would still be necessary for the organisms to have some mechanism to avoid gliding away from the euphotic zone (i.e., indefinitely downward), explanations that are in complete agreement with the observations are not obvious to us. A positive light response operating at lower thresholds that would tend to keep the lower boundary of the blue-green layer away from darkness would not explain why the lower boundary did not significantly rise at dusk. Again, some sort of chemotactic response(s) may be the explanation (22, 37).

Since the mat as a whole became anoxic and sulfide-rich at night, and since the migrating *Oscillatoria-Spirulina* assemblage was capable of exclusive anoxygenic photosynthesis in the presence of 0.6 mM sulfide, it is likely that early morning photosynthesis was anoxygenic. Anoxygenic photosynthesis probably proceeded on the mat surface until reduced levels of sulfide permitted oxygenic photosynthesis to commence and, perhaps, relieve chemotactic responses due to sulfide. A similar case has been described for *Oscillatoria* cf. *boryana* in mats of warm springs (5). However, there is as yet no rigorous evidence that sulfide must be depleted before downward migration can occur.

**Conclusions.** In this paper we describe and quantify the in situ diel migration patterns of some microorganisms with levels of resolution of approximately 0.1 mm in some cases. Coupled

with available microsensor technology, our findings allowed us to test our hypothesis regarding cyanobacterial migration in natural benthic ecosystems (i.e., that vertical migration is a strategy combining photoprotection and optimization of the photosynthetic environment). This could be demonstrated in this 28-h diel study, but whether this is a phenomenon that is restricted to this particular mat or a general pattern in cyanobacterial soft mats worldwide remains to be determined. Our findings underscore the importance of migratory activity in the biology and functioning of benthic microbial assemblages. The presence of migration should be considered a possibly important variable in many future ecophysiological studies.

#### ACKNOWLEDGMENTS

We thank D. J. Des Marais for organizing the field trips to Guerrero Negro and providing travel funds to F.G.-P. We are grateful to B. K. Pierson for lending us her fiber optic microsensor and for help with the measurements. Incident irradiance data were kindly provided by L. Prufert-Bebout, B. Bebout, and H. Paerl. Comments by B. Bebout, L. Prufert-Bebout, M. Kühl, and an anonymous reviewer improved the manuscript.

This work was supported by NSF grant BSR-8906739 to R.W.C.

#### REFERENCES

- Agel, G., W. Nultsch, and E. Rhiel. 1987. Photoinhibition and its wavelength dependence in the cyanobacterium *Anabaena variabilis*. *Arch. Microbiol.* **147**:370-374.
- Carr, N. G., and M. Wyman. 1986. Cyanobacteria: their biology in relation to oceanic picoplankton. *Can. Bull. Fish. Aquat. Sci.* **214**:159-204.
- Castenholz, R. W. 1968. The behavior of *Oscillatoria terebriformis* in hot springs. *J. Phycol.* **4**:132-139.
- Castenholz, R. W. 1982. Motility and taxes, p. 413-440. In N. G. Carr and B. A. Whitton (ed.), *The biology of cyanobacteria*. Blackwell Scientific Publishers, Oxford.
- Castenholz, R. W., B. B. Jørgensen, E. D'Amelio, and J. Bauld. 1991. Photosynthetic and behavioral versatility of the cyanobacterium *Oscillatoria boryana* in a sulfide-rich microbial mat. *FEMS Microbiol. Ecol.* **86**:45-58.
- Cline, J. D. 1969. Spectrophotometric determination of hydrogen sulfide in natural waters. *Limnol. Oceanogr.* **14**:454-458.
- Cohen, Y., R. W. Castenholz, and H. O. Halvorson (ed.). 1984. *Microbial mats: stromatolites*. Alan R. Liss, New York.
- Cohen, Y., and E. Rosenberg (ed.). 1989. *Microbial mats. Physiological ecology of benthic microbial communities*. American Society for Microbiology, Washington, D.C.
- Garcia-Pichel, F. 1989. Rapid bacterial swimming measured in swarming cells of *Thiovulum majus*. *J. Bacteriol.* **171**:3560-3563.
- Garcia-Pichel, F., and R. W. Castenholz. 1990. Comparative anoxygenic photosynthetic capacity in 7 strains of a thermophilic cyanobacterium. *Arch. Microbiol.* **153**:344-351.
- Garcia-Pichel, F., and R. W. Castenholz. 1991. Characterization and biological implications of scytonemin, a cyanobacterial sheath pigment. *J. Phycol.* **27**:395-409.
- Garcia-Pichel, F., N. D. Sherry, and R. W. Castenholz. 1992. Evidence for a UV sunscreen role of the extracellular pigment scytonemin in the terrestrial cyanobacterium *Chlorogloeopsis* spp. *Photochem. Photobiol.* **56**:17-23.
- Haxo, F. T., and L. R. Blinks. 1950. Photosynthetic action spectra of marine algae. *J. Gen. Physiol.* **33**:389-392.
- Jagger, J. 1985. *Solar-UV actions on living cells*, Praeger, New York.
- Javor, B. 1989. *Hypersaline environments*, Springer Verlag, Berlin.
- Jørgensen, B. B., Y. Cohen, and D. J. Des Marais. 1987. Photosynthetic action spectra and adaptation to spectral light distribution in a benthic cyanobacterial mat. *Appl. Environ. Microbiol.* **53**:879-886.
- Jørgensen, B. B., and D. J. Des Marais. 1988. Optical properties of benthic photosynthetic communities: fiber-optic studies of cy-

- nobacterial mats. *Limnol. Oceanogr.* **33**:99–113.
18. **Jørgensen, B. B., and N. P. Revsbech.** 1983. Colorless sulfur bacteria, *Beggiatoa* spp. and *Thiovulum* spp. in O<sub>2</sub> and H<sub>2</sub>S microgradients. *Appl. Environ. Microbiol.* **45**:1261–1270.
  19. **Kühl, M., and B. B. Jørgensen.** 1992. Spectral light measurements in microbenthic phototrophic communities with a fiber-optic microprobe coupled to a sensitive diode array detector. *Limnol. Oceanogr.* **37**:1813–1823.
  20. **Lassen, C.** Personal communication.
  21. **Lassen, C., H. Ploug, and B. B. Jørgensen.** 1992. Microalgal photosynthesis and spectral scalar irradiance in coastal marine sediments of Limfjorden, Denmark. *Limnol. Oceanogr.* **37**:760–762.
  22. **Malin, G., and A. E. Walsby.** 1985. Chemotaxis of a cyanobacterium on concentration gradients of carbon dioxide, bicarbonate and oxygen. *J. Gen. Microbiol.* **131**:2643–2652.
  23. **Mir, J., M. Martínez-Alonso, I. Esteve, and R. Guerrero.** 1991. Vertical stratification and microbial assemblage of a microbial mat in the Ebro Delta (Spain). *FEMS Microbiol. Ecol.* **86**:59–68.
  24. **Møller, M. M., L. P. Nielsen, and B. B. Jørgensen.** 1985. Oxygen responses and mat formation by *Beggiatoa* sp. *Appl. Environ. Microbiol.* **50**:373–382.
  25. **Nelson, D. C., and R. W. Castenholz.** 1981. Use of reduced sulfur compounds by *Beggiatoa* sp. *J. Bacteriol.* **147**:140–154.
  26. **Nelson, D. C., N. P. Revsbech, and B. B. Jørgensen.** 1986. Microoxic-anoxic niche of *Beggiatoa* spp.: microelectrode survey of marine and freshwater strains. *Appl. Environ. Microbiol.* **52**:161–168.
  27. **Nicholson, J. M., J. F. Stolz, and B. K. Pierson.** 1987. Structure of a microbial mat at Great Sippewissett Marsh, Cape Cod, Massachusetts. *FEMS Microbiol. Ecol.* **45**:343–364.
  28. **Pentecost, A.** 1984. Effects of sedimentation and light intensity on mat-forming *Oscillatoriaceae* with particular reference to *Microcoleus lyngbyaceus* Gomont. *J. Gen. Microbiol.* **130**:983–990.
  29. **Pierson, B. K., and H. M. Howard.** 1972. Detection of bacteriochlorophyll-containing microorganisms by infrared fluorescence microscopy. *J. Gen. Microbiol.* **73**:359–363.
  30. **Pierson, B. K., A. Oesterle, and G. L. Murphy.** 1987. Pigments, light penetration and photosynthetic activity in the multi-layered microbial mats of Great Sippewissett Salt Marsh, Massachusetts. *FEMS Microbiol. Ecol.* **45**:365–376.
  31. **Pierson, B. K., V. M. Sands, and J. L. Frederick.** 1990. Spectral irradiance and distribution of pigments in a highly layered microbial mat. *Appl. Environ. Microbiol.* **56**:2327–2340.
  32. **Ploug, H., C. Lassen, and B. B. Jørgensen.** 1993. Action spectra of microalgal photosynthesis and depth distribution of spectral scalar irradiance in a coastal marine sediment of Limfjorden, Denmark. *FEMS Microbiol. Ecol.* **102**:261–270.
  33. **Revsbech, N. P., and B. B. Jørgensen.** 1983. Photosynthesis of benthic microflora measured with high spatial resolution by the oxygen microprofile method: capabilities and limitations of the method. *Limnol. Oceanogr.* **28**:749–756.
  34. **Revsbech, N. P., and B. B. Jørgensen.** 1986. Microelectrodes: their use in microbial ecology, p. 293–352. *In* K. C. Marshall (ed.), *Advances in microbial ecology*. Plenum Press, New York.
  35. **Revsbech, N. P., B. B. Jørgensen, T. H. Blackburn, and Y. Cohen.** 1983. Microelectrode studies of the photosynthesis and O<sub>2</sub>, H<sub>2</sub>S and pH profiles of a microbial mat. *Limnol. Oceanogr.* **28**:1062–1074.
  36. **Richardson, L. L., and R. W. Castenholz.** 1987. Diel vertical movements of the cyanobacterium *Oscillatoria terebriformis* in a sulfide-rich microbial mat. *Appl. Environ. Microbiol.* **53**:2142–2150.
  37. **Richardson, L. L., and R. W. Castenholz.** 1989. Chemokinetic motility responses of the cyanobacterium *Oscillatoria terebriformis*. *Appl. Environ. Microbiol.* **55**:261–263.
  38. **Simon, R. D.** 1981. Gliding motility in *Aphanathece halophytica*: analysis of wall proteins in *mot* mutants. *J. Bacteriol.* **148**:315–321.
  39. **Sokal, R. S., and F. J. Rohlf.** 1981. *Biometry*. W. H. Freeman & Co., New York.
  - 39a. **Staley, J. T., M. P. Bryant, N. Pfennig, and J. G. Holt (ed.).** 1989. *Bergey's manual of systematic bacteriology*, vol. 3. Williams & Wilkins, Baltimore.
  40. **Whale, G. F., and A. E. Walsby.** 1984. Motility of the cyanobacterium *Microcoleus chthonoplastes* in mud. *Br. Phycol. J.* **19**:117–123.
  41. **Whitelam, G. C., and G. A. Codd.** 1986. Damaging effects of light on microorganisms, p. 129–169. *In* R. A. Herbert and G. A. Codd (ed.), *Microbes in extreme environments*. Academic Press, London.